Journal of Power Sources 220 (2012) 79–83

Contents lists available at SciVerse ScienceDirect

Journal of Power Sources

journal homepage: www.elsevier.com/locate/jpowsour

Short communication

Enhancement of proton exchange membrane fuel cell performance by doping microporous layers of gas diffusion layers with multiwall carbon nanotubes

Rüdiger Schweiss [a,*], Marcus Steeb [a], Peter M. Wilde [a], Tim Schubert [b]

[a] SGL Carbon GmbH, Werner-von-Siemensstrasse 18, 86405 Meitingen, Germany
[b] FutureCarbon GmbH, Gottlieb-Keim-Strasse 60, 95448 Bayreuth, Germany

HIGHLIGHTS

- Microporous Layers (MPLs) doped with Multiwall Carbon Nantotubes.
- MWCNT generate a particular pore size distribution of the MPL.
- Excellent PEMFC performance was observed for the MWCNT-doped MPLs.

ARTICLE INFO

Article history:
Received 30 April 2012
Received in revised form
17 July 2012
Accepted 26 July 2012
Available online 3 August 2012

Keywords:
Carbon nanotubes
Gas diffusion layer
PEM fuel cell
Microporous layers

ABSTRACT

Microporous layers (MPLs) of gas diffusion layers (GDLs) were modified by multiwall carbon nanotubes (MWCNTs) using a wet-chemical approach. Carbon nanotubes were dispersed along with other MPL components and coated onto a GDL backing. The electronic resistance of the GDL was significantly reduced by the addition of MWCNTs. A larger mean pore diameter was obtained as compared to the reference substrates. The improved performance of proton exchange membrane fuel cells (PEMFCs) using such CNT-doped GDLs is attributed to a lower electronic resistance along with improved mass transport. Synergy effects of different carbon materials with MWCNTs and advanced dispersion processes were found to play a key role in achieving the performance improvements.

1. Introduction

Proton exchange membrane fuel cells (PEMFCs) rank among the prominent candidates intended to replace fossil fuel-based power sources in stationary and mobility applications. Particular viability of PEMFCs is seen in the field of emission-free vehicle propulsion, where significant achievements have already been made [1,2]. Due to space restrictions in automotive fuel cell systems, a further reduction in the stack size by improving the achievable power density is desirable. Apart from operating conditions, efficiency and loading of noble-metal catalysts, the voltage losses associated with the ohmic resistances and the reactand supply constitute limiting factors for the power density.

Gas diffusion layers (GDLs) deserve particular attention since their function in PEMFCs implies all relevant transport processes with regard to electricity, heat, fuel gases, liquid water and water vapour [3–5]. A recent review provides an in-depth insight into the structure–property relationships of gas diffusion layers [6].

It is generally understood that a bi-component gas diffusion medium consisting of a macroporous carbon fibre backing (carbon papers, 3D-nonwoven fabrics or cloths) covered with a microporous layer (MPL) coating is the preferable gas diffusion medium for PEMFCs [7–9]. This is due to the fact that this particular structure with a graded porosity (backing around 80–90% and MPL around 20%) is capable of managing the delicate balance of maintaining an appropriate hydration level of the proton exchange membrane and the catalyst layers while at the same time actively supporting the release of excess water through the GDL into the flow field channels [6,10]. Additionally, microporous layers are known to provide a low contact resistance between the GDL and the catalyst sites and efficiently protect the proton-exchange membrane from perforation by the carbon fibres.

Microporous layers commonly consist of a carbon black matrix held together by a fluorinated polymer binder, which, in addition, produces hydrophobic properties which are indispensable for the functions stated above. Preparation of MPLs is mainly performed by

* Corresponding author. Tel.: +49 8271 83 1702; fax: +49 8271 83101702.
E-mail address: ruediger-bernd.schweiss@sglcarbon.de (R. Schweiss).

0378-7753/$ – see front matter © 2012 Elsevier B.V. All rights reserved.
http://dx.doi.org/10.1016/j.jpowsour.2012.07.078

blade coating or screen-printing of aqueous dispersion of carbon black/fluoropolymer. It is generally accepted that a bimodal pore size distribution in the microporous layer is beneficial for water management since concomitant water and gas transport are highly efficient in this case.

Further improvement of the GDL water management capability has been addressed by GDL/MPL modifications such as perforation [11,12], pore size adjustment [13], addition of pore formers [14], porosity gradients in the MPLs [15] or hydrophilic microfibres [16,17]. These approaches, however, add complexity in terms of manufacturing or might be generated at the expense of electronic conductivity or fuel cell durability.

Carbon nanotubes (CNTs) are widely regarded as materials with excellent conductivities with respect to electricity and heat [18,19], together with a large surface area and electrocatalytic properties. Electrical percolation in matrix systems or composites, using MWCNTs as conductive additives can be achieved with very small quantities [20,21] compared to other carbon materials. As a matter of fact, applications of these materials in electrochemical power sources seem imperative. The preliminary use of carbon nanotubes in PEMFCs has been reported with respect to catalyst supports [22–26] or catalyst substitutes [27]. The use of single wall nanotube (SWCNT) modified GDLs and Pt/MWCNT catalysts has been investigated by Kannan et al. [28]. They observed excellent PEMFC performance owing to enhanced Pt activity. Moreover, there is evidence that carbon nanotubes exhibit superior corrosion resistance as compared to common catalyst supports based on carbon blacks [29].

Studies on MWCNTs as functional components in microporous layers are scarce. Gharibi et al. [30] prepared gas diffusion electrodes (GDEs) using MWCNT and a high surface area carbon black (Vulcan XC72). Chronopotentiometry of these GDEs showed improved catalyst utilisation when MWCNTs are added. Purwanto et al. [31] prepared MPLs from Vulcan black and SWCNTs and MWCNTs and observed improved fuel cell performance in the resistance-controlled current regime.

This study was dedicated to exploring the potential of carbon nanotubes as a functional component in the bulk of the microporous layer of commercially manufactured gas diffusion layers used in PEMFCs. Materials were produced on an industrial scale using only aqueous coating inks which were prepared using a novel, proprietary method. Materials were investigated using single cell PEMFC tests with particular emphasis on automotive conditions (high current densities and wet gases).

2. Experimental

MWCNTs were synthesized by means of CCVD (catalytic assisted chemical vapour deposition) process. High-quality MWCNTs from FutureCarbon GmbH, namely with easily unravelable entanglements and agglomerates, set the stage for achieving the targeted properties of the MWCNT-carbon black dispersion. To adjust the rheological properties of the carbon black/MWCNT dispersion, hydroxyethyl cellulose was added. Finally, aqueous polytetrafluoroethylene (PTFE) dispersion was added in order to obtain a coating ink. The fraction of MWCNT in the carbon matrix of the MPL (χ) is given by

$$\chi_{\mathrm{CNT}}^{\mathrm{MPL}}\ (\%) = 100 \cdot \left(\frac{m_{\mathrm{CNT}}}{m_{\mathrm{CNT}} + m_{\mathrm{CB}}} \right) \quad (1)$$

where m are the masses of carbon nanotubes (CNT) and the carbon black (CB) in the MPL, respectively. The carbon paste was coated onto rolls of GDL backings consisting of 2D-nonwovens (carbon paper-type, Sigracet® GDL 25 BA, thickness 0.19 mm) and 3D nonwovens (carbon nonwoven-fabric, Sigracet® GDL 10 BA, thickness 0.40 mm) using a production-scale blade coating machine and was subsequently sintered.

Electronic resistance measurements were conducted by means of 2-point (through-plane) and 4-point probes (in-plane) using gold-plated contacts [3]. The in-plane resistances reported in this paper constitute averages over the resistances determined for the machine-direction of the backing and the cross-machine direction. A compression load of 1 MPa was applied during the measurements. Pore characteristics were analysed by means of capillary flow porosimetry (Porous Materials Inc., USA) and mercury intrusion (Quantachrome, Germany). Liquid water permeability (through plane) was determined by means of a PMI liquid permeameter (Porous Materials Inc., USA). Single cell PEMFC tests were performed with a 25 cm^2 test cell (Baltic Fuel Cells, Germany) using a fully automated fuel cell test bench (Greenlight, Canada). The GDLs were pressed against graphite flow fields with a compression load of 1 MPa. A commercial catalyst-coated membrane (W.L. Gore, Germany) with a total Pt loading of 0.5 mg cm^{-2} was used for all fuel cell tests. Stoichiometries during operation were 1.5 (H_2) and 2.5 (air) respectively. Inlet pressure was 50 kPa. The data presented in this paper constitute average values for 3 samples of each GDL type characterised with 6 consecutive polarization curves.

3. Results and discussion

3.1. Electronic properties

Fig. 1 shows the electronic resistances (through-plane and in-plane) of reference GDLs (Sigracet® GDL 25 BC, GDL 10 BC) and

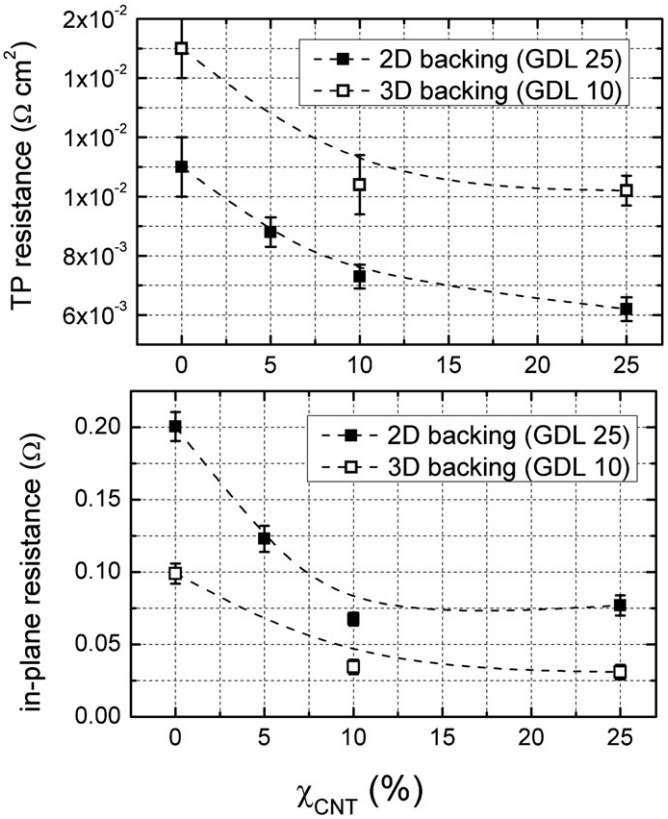

Fig. 1. Through-plane (R_{TP}, top) and in-plane (R_{IP}, bottom) electronic resistance of gas diffusion layers containing various amounts of MWCNT in the microporous layer for carbon paper-based GDLs (platform GDL 25) and 3D-carbon nonwoven fabric-based GDLs (platform GDL 10).

GDLs with addition of MWCNT to the carbon matrix of the microporous layers. A significant reduction in the resistances (up to 50%) is achieved by the addition of carbon nanotubes, especially for the in-plane direction. This might be attributed to the high surface area and the high aspect ratio of the MWCNTs, which provide a large number of electronic pathways between the carbon black-PTFE matrix of the MPL and the fibre skeleton of the GDL backing.

The electronic resistances, however, level off when the CNT content is increased from 10% to 25%. This is likely due to the fact that the aforementioned effect is overcompensated by the decreasing density of the MPL (see next chapter).

3.2. Pore characteristics and liquid water transport

Table 1 shows the results of detailed pore analyses of the materials. The materials were investigated by means of capillary flow porosimetry (CFP), which probes flow pores down to a pore diameter of 0.8 μm, and mercury intrusion porosimetry (MIP) which covers the total range of porosity. Both techniques show that the mean pore diameters are larger when MWCNTs are added to the microporous layer. This is also reflected by the higher gas permeabilities. Mercury intrusion porosimetry reveals a large reduction of pores with diameters <1 μm as compared to the reference materials. This particular microstructure might be generated by the adsorption of MWCNTs on the carbon black surface, which act as spacers that prevent the coalescence of carbon black particles. By contrast, the total porosity of the materials remains almost constant.

Water transport through GDLs is known to take place as a two-phase flow process. The water release properties of gas diffusion media are important, especially at high current density operation, in order to avoid flooding of the catalyst sites and blocking of the GDL backings, which both result in lower catalyst utilisation and in increased mass-transport overpotentials. Liquid water removal therefore appears to make a significant contribution and this has been verified by means of GDL materials which contain hydrophilic water sinks in the MPL [16,17]. In addition, it was observed that the CNT-doped MPLs which display a larger mean pore size than the reference material (25 BC) show a significantly enhanced liquid permeability (factor of around 10, Table 1). As there are no differences with regard to total porosity, the increased gas permeability of MWCNT-doped MPLs indicates a lower tortuosity.

3.3. Fuel cell testing

Fig. 2 shows the polarization curves of PEMFC single cells under wet conditions (100% relative humidity, cell temperature 70 °C) employing CNT-modified GDLs and corresponding reference materials from the two GDL platforms (carbon paper = 2D and carbon nonwoven fabric = 3D). The increased conductivity of the MWCNT-doped GDLs is reflected by a slightly flatter slope of the linear part of the polarization curves (0.5–1.0 A cm^{-2}). A simple description (neglecting the anode overpotentials) of the polarization curves (E_{cell} versus current density j) is given by Eq. (2) [32]

$$E_{cell} = E_{rev} - b\cdot\log\left[\frac{j}{j_0}\right] - j\cdot ASR - 2.303\frac{RT}{F}\log\left[1-\frac{j}{j_L}\right] \quad (2)$$

where ASR represents the area-specific ohmic resistances (ionic and electronic resistances), b the (cathodic) Tafel slope and j_L the limiting current density. The differences in the ohmic resistance contributions (ASR) to the polarization curves reflect the lower through-plane resistances of the GDL materials (Fig. 1, Table 2). Additionally, higher limiting current densities are observed for the CNT-doped MPLs.

Applying an approach proposed by Fenton and Popov et al. [10,33,34], "empiric" Tafel slopes (b_e) are obtained plotting the ASR-corrected cell potential versus the logarithm of the "kinetic" current density (j_{kin})

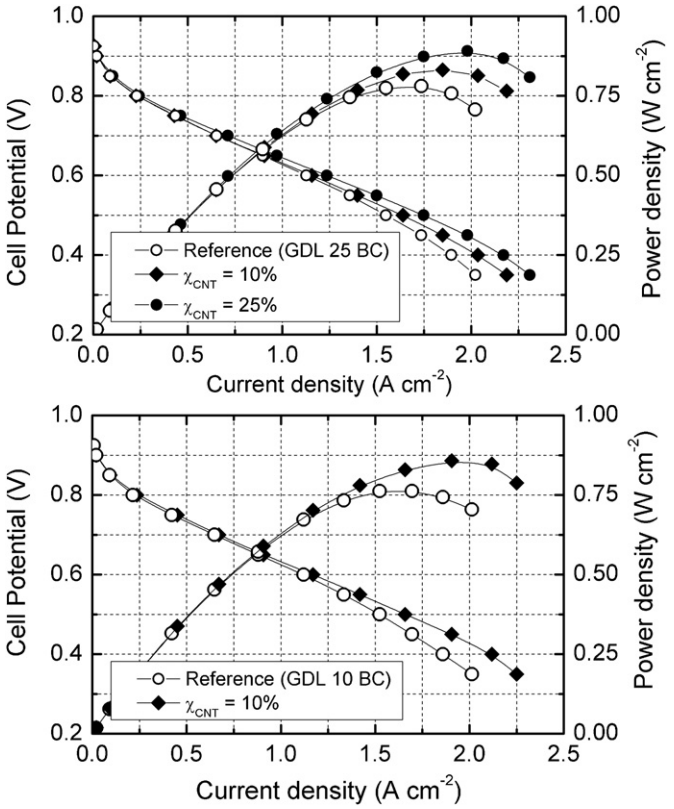

Fig. 2. Polarization curves (average of three samples in each case) of various GDL grades containing MWCNT-doped microporous layers and corresponding reference systems at a cell temperature of 70 °C and 100% relative humidity using GDL backings of carbon paper (top) and 3D-carbon nonwoven fabric (bottom). Stoichiometries: 1.5 (H_2) and 2.5 (air).

Table 1
Pore characteristics obtained from capillary flow porosimetry (CFP), mercury intrusion porosimetry (MIP) and liquid permeability of carbon paper (Sigracet® GDL 25 BC) gas diffusion layers containing various amounts of MWCNTs (χ_{CNT}) in the carbon matrix of the microporous layer.

GDL 25 BC with addition of	0% MWCNT	10% MWCNT	25% MWCNT
Gas permeability ($cm^3\ cm^{-2}\ s^{-1}$)	1.0	4.0	7.7
Liquid water permeability ($10^{-12}\ m^2$)	0.1	1.2	1.4
CFP			
Bubble point (CFP) in μm	28	39	45
Mean pore diameter (μm)	4.2	4.4	8.0
MIP			
Mean pore diameter (μm)	0.1	0.34	0.35
Total porosity (%)	41	40	40

Table 2
Area-specific resistances (ASR) and empiric Tafel slopes (b_e) calculated from polarization curves (Fig. 2).

	ASR (Ω cm^2)	b_e (mV dec^{-1})
GDL 25 BC (0% MWCNT)	0.169	104
GDL 25 BC (10% MWCNT	0.159	96
GDL 25 BC (25% MWCNT)	0.154	64
GDL 10 BC (0% MWCNT)	0.175	107
GDL 10 BC (10% MWCNT)	0.167	63

$$j_{kin} = \frac{j}{(1 - j/j_L)} \quad (3)$$

and fitting only the part with the steeper slope ($i_{kin} > 1$ A cm^{-2}) [32,33]. This assumption is valid for first order oxygen reduction kinetics and negligible anode overpotentials. As revealed in Table 2, the lower empiric Tafel slopes (b_e) obtained after transformation of the polarization curves indicate significantly enhanced oxygen diffusion within the catalyst layers [35]. Hence, the beneficial effect of the CNT-doped MPL is expected to be due to lower water saturation at the MPL/catalyst interface.

Previous investigations suggest a simple correlation between the GDL porosity and the oxygen diffusion in the gas diffusion medium [36] which, in turn, is closely related to the mass-transfer overpotentials and the limiting current density. Moreover, a bimodal pore size distribution was concluded to sustain effective water management [15]. These concepts, however, cannot be applied here, since the total porosities of all GDLs studied were almost identical and the pore size distributions were much more even for the CNT-modified MPLs. The latter, however, showed significantly larger limiting currents as compared to the reference MPLs.

An experimental study [37] has recently demonstrated that the Bruggeman correction [38–40] underestimates the tortuosity for the calculation of oxygen diffusivity. This means that the larger limiting currents for the CNT-doped MPLs might be due to a less tortuous MPL structure.

Additionally, the enhanced liquid water permeability of the MWCNT-doped MPLs, which is due to a larger number of small macropores (see Table 1), is expected to support water management of the PEMFC at larger current densities under wet conditions. Kong et al. [41] reported similar observations for GDLs with tuned MPL pore sizes, where an increased amount of small macropores (diameter < 10 μm) in the MPL results in better PEMFC performance.

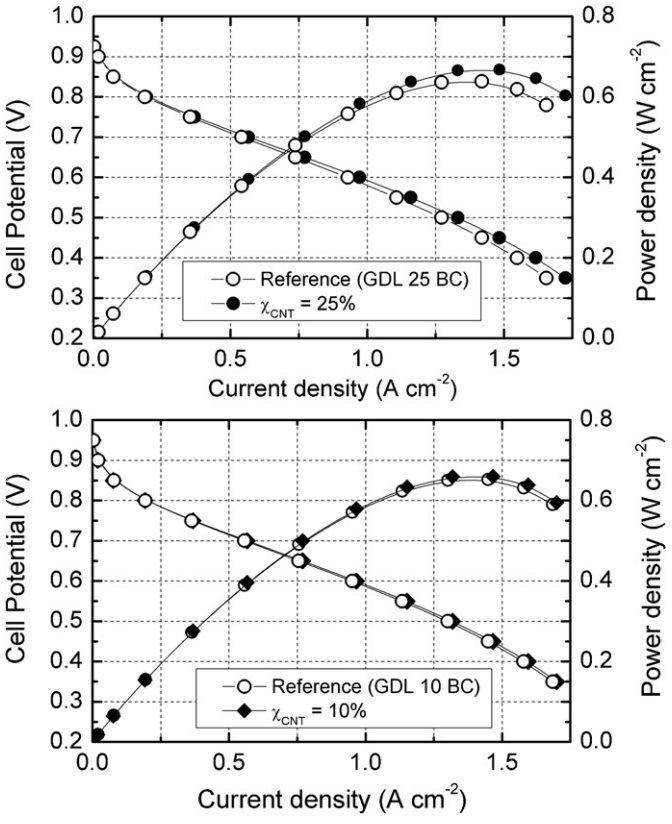

Fig. 3. Polarization curves (average of three samples in each case) of various GDL grades containing MWCNT-doped microporous layers and corresponding reference systems at a cell temperature of 80 °C and 40% relative humidity using GDL backings of carbon paper (top) and 3D-carbon nonwoven fabric (bottom). Stoichiometries: 1.5 (H_2) and 2.5 (air).

Single-cell PEMFC tests under dry conditions were performed as a reference. Fig. 3 shows selected polarization curves of MWCNT-doped MPLs for the 2D and 3D backings including unmodified reference materials. In contrast to wet operation, the differences in the power densities between standard MPLs and MWCNT-doped MPLs are negligible. This might be seen as another indication of the beneficial role of MWCNTs on water management since under dry operation, the performance-limiting factor is most likely the dry-out of the proton-exchange membrane.

4. Conclusions

Gas diffusion layers comprising bi-component microporous layers (carbon black and MWCNTs) show superior fuel cell performance as compared to the corresponding reference materials. This has to be attributed to a synergetic effect of increased electronic conductivity coupled with a particular MPL structure which is generated by the addition of well-dispersed MWCNTs. MWCNT-doped microporous layers exhibit increased gas and liquid water transport capabilities, thus mitigating losses which are associated with oxygen deficiency. The advanced transport properties are most likely due to a more favourable pore size distribution and to structural synergy effects of the carbon materials with MWCNTs.

Further insights into these effects might be inferred from capillary pressure, diffusivity and in situ imaging studies of water transport which are currently underway [42].

Combined with other novel fuel cell components, such as carbon nanomaterial-based catalysts, this straightforward approach has the potential to substantially contribute to the commercialization of PEMFC technology in mobility applications.

Acknowledgement

This study was funded by the German Federal Ministry of Education and Research (BMBF) within the InnoCNT cluster initiative (contract no. X3044E). Fruitful discussions with Dr Egbert Figgemeier (Bayer Technology Services, Leverkusen) are gratefully acknowledged.

References

[1] P. Mock, S.A. Schmid, J. Power Sources 190 (2009) 133–140.
[2] F. Barbir, S. Yazici, Int. J. Energy Res. 32 (2008) 369–378.
[3] S. Park, J.-W. Lee, Int. J. Hydrogen Energy 37 (2012) 5850–5865.
[4] M.F. Mathias, J. Roth, J. Fleming, W. Lehnert, in: W. Vielstich, H.A. Gasteiger, A. Lamm (Eds.), Handbook of Fuel Cells – Fundamentals Technology and Applications, vol. 3, Wiley, New York, 2003 (Chapter 6).
[5] L. Cindrella, A.M. Kannan, J.F. Lin, K. Saminathan, Y. Ho, C.W. Lin, J. Wertz, J. Power Sources 194 (2009) 146–160.
[6] S. Park, J.-W. Lee, B.N. Popov, Int. J. Hydrogen Energy 37 (2012) 5850–5865.
[7] J.T. Gostick, M.A. Ioannidis, M.W. Fowler, M.D. Pritzker, Electrochem. Commun. 11 (2009) 576–579.
[8] A.Z. Weber, J. Newman, J. Electrochem. Soc. 152 (2005) A677–A688.
[9] S.G. Kandlikar, Z. Lu, J. Fuel Cell Sci. Technol. 6 (2009) 1–13.
[10] S. Park, J.-W. Lee, B.N. Popov, J. Power Sources 177 (2008) 457–463.
[11] M.P. Manahan, M.C. Hatzell, E.C. Kumbur, M.M. Mench, J. Power Sources 196 (2011) 5573–5582.
[12] E.E. Kimball, J.B. Benziger, Y.G. Kevrekidis, Fuel Cells 10 (2010) 530–544.
[13] S. Park, J.-W. Lee, B.N. Popov, J. Power Sources 163 (2006) 357–363.
[14] J.H. Chun, K.T. Park, D.H. Jo, J.Y. Lee, S.G. Kim, S.H. Park, E.S. Lee, J.-Y. Jyoung, S.H. Kim, Int. J. Hydrogen Energy 36 (2011) 8422–8428.
[15] G. Selvarani, A.K. Sahu, P. Sridhar, S. Pitchumani, A.K. Shukla, J. Appl. Electrochem. 38 (2008) 357–362.
[16] R. Schweiss, M. Steeb, P.M. Wilde, Fuel Cells 10 (2010) 1176–1180.

[17] R. Mukundan, J.R. Davey, J.D. Fairweather, D. Spernjak, J. Spendelow, D.S. Hussey, D.L. Jacobson, P. Wilde, R. Schweiss, R.L. Borup, ECS Trans. 33 (2010) 1109–1114.
[18] M.S. Dresselhaus, G. Dresselhaus, P. Avouris (Eds.), Carbon Nanotubes: Synthesis, Structure, Properties, and Applications, Springer, N.Y., 2000.
[19] P.M. Ajayan, Chem. Rev. 99 (1999) 1787.
[20] M. Okada, Y. Konta, N. Nakagawa, J. Power Sources 185 (2008) 711–716.
[21] C.A. Martin, J.K.W. Sandler, M.S.P. Shaffer, Compos. Sci. Technol. 64 (2004) 2309–2316.
[22] J.K.W. Sandler, J.E. Kirk, I.A. Kinloch, M.S.P. Shaffer, A.H. Windle, Polymer 44 (2003) 5893–5899.
[23] P. Wu, B. Li, H. Du, L. Gan, F. Kang, Y. Zeng, J. Power Sources 184 (2008) 381–384.
[24] C. Wang, M. Waje, X. Wang, J.M. Tang, R.C. Haddon, Y. Yan, Nano Lett. 4 (2004) 345–348.
[25] C.C. Chen, C.F. Chen, C.H. Hsu, I. Li, Diam. Relat. Mater. 14 (2005) 770–773.
[26] M. Söhn, M. Lebert, T. Wirth, S. Hoffmann, N. Nicoloso, J. Power Sources 176 (2008) 494–498.
[27] S. Wang, D. Yu, L. Dai, J. Am. Chem. Soc. 133 (2011) 5182–5185.
[28] A.M. Kannan, V.P. Veedu, L. Munukutla, M.N. Ghasemi-Nejhad, Electrochem. Solid State Lett. 10 (2007) B47–B50.
[29] Y. Shao, G. Yin, J. Zhang, H. Xu, X. Zhu, J. Chen, Electrochim. Acta 51 (2006) 5853–5857.
[30] H. Gharibi, M. Javaheri, R.A. Mirzaie, Int. J. Hydrogen Energy 35 (2010) 9241–9251.
[31] W.W. Purwanto, V.J. Wargadalam, B. Pranoto, Int. J. Electrochem. Sci. 7 (2012) 525–533.
[32] A.Z. Weber, J. Newman, Chem. Rev. 104 (2004) 4679–4726.
[33] M.V. Williams, H.R. Kunz, J.M. Fenton, J. Electrochem. Soc. 152 (2005) A635–A644.
[34] S. Park, B.N. Popov, Fuel 88 (2009) 2068–2073.
[35] M.L. Perry, J. Newman, E.J. Cairns, J. Electrochem. Soc. 145 (1998) 5–15.
[36] S. Park, B.N. Popov, Electrochim. Acta 54 (2009) 3473–3479.
[37] Z. Yu, R.N. Carter, J. Power Sources 195 (2010) 1079–1084.
[38] H. Tang, S. Wang, M. Pan, R. Yuan, J. Power Sources 166 (2007) 41–46.
[39] J.H. Nam, M. Kaviany, Int. J. Heat Mass Transfer 46 (2003) 4595–4611.
[40] J.G. Pharoah, K. Karan, W. Sun, J. Power Sources 161 (2006) 214–224.
[41] C.S. Kong, D.Y. Lim, H.K. Lee, Y.G. Shul, T.H. Lee, J. Power Sources 108 (2002) 185–191.
[42] D. Spernjak, R. Mukundan, P. Wilde, R. Schweiss, K.L. More, D. Langlois, J. Fairweather, R.L. Borup, ECS Trans., submitted for publication.